RESEARCH ARTICLE
doi: 10.2306/scienceasia1513-1874.2024.075

ScienceAsia 50 (4): 2024: ID 2024075: **1–10**

CO_2-brine-rock interactions in Permian carbonate formations, North-eastern Thailand

Thitiphan Assawincharoenkij[a,b], Piyaphong Chenrai[a,b,c,*], Sukonmeth Jitmahantakul[b,c], Falan Srisuriyachai[d], Soraya Suninbun[a], Kanit Laosritrakul[a], Chawisa Phujareanchaiwon[e]

[a] Applied Mineral and Petrology Special Task Force for Activating Research (AMP STAR), Department of Geology, Faculty of Science, Chulalongkorn University, Bangkok 10330 Thailand

[b] Basin Analysis and Structural Evolution Research Unit (BASE RU), Department of Geology, Faculty of Science, Chulalongkorn University, Bangkok 10330 Thailand

[c] MSc Program in Petroleum Geoscience, Faculty of Science, Chulalongkorn University, Bangkok 10330 Thailand

[d] Department of Mining and Petroleum Engineering, Faculty of Engineering, Chulalongkorn University, Bangkok 10330 Thailand

[e] Department of Earth Sciences, Faculty of Science, Kasetsart University, Bangkok 10900 Thailand

[*]Corresponding author, e-mail: Piyaphong.c@chula.ac.th

Received 9 May 2023, Accepted 9 May 2024
Available online 20 Aug 2024

ABSTRACT: This study described the results of carbon dioxide-brine-rocks interactions of carbonate rock samples from the Pha Nok Khao (PNK) and the Huai Hin Lat (HHL) Formations in Thailand. The aim of this study was to investigate geochemical and physical changes in carbonate formations commonly used for long-term storage of carbon dioxide (CO_2). The samples were classified into five lithological facies: fractured limestone, grained limestone, mud limestone, dolomite, and sandstone. The mineral compositions and textures of the samples were analyzed by using petrography, X-ray diffraction (XRD), X-ray fluorescence (XRF), and Inductively Coupled Plasma-Optical Emission Spectrometer (ICP-OES). The results revealed changes in geochemical and physical properties after soaking the samples in CO_2-dissolved brine water. When exposed to low pH CO_2-brine water, mineral compositions in carbonate rocks such as dolomite, quartz, and calcite undergo dissolution, leading to increased porosity. The study identified lithology, formation of brine water, and effective porosity as key control factors in CO_2-brine-rock interactions. The findings suggested that long-term CO_2 storage in the PNK carbonate reservoirs might not be useful due to its potential dissolution in an acidic environment. The dissolution could affect the bulk porosity and strength of the reservoir formation leading to fracture failure after hundreds of years of CO_2 injection. This study had implications on the feasibility of carbon capture and storage strategies, highlighting the need for further investigation and consideration of alternative storage options.

KEYWORDS: geological carbon storage, limestone, dolomite, geochemical analysis, porosity

INTRODUCTION

Similar to the rest of the world, the consumption of fossil fuels in Thailand takes up 79% of the total energy due to rapid growth in industrialization and modernization leading to an increase in the demand for energy [1]. The consumption of fossil fuels such as coal, oil, and natural gas results in a large amount of CO_2 emission into the atmosphere causing air pollution and global warming problems [1–4]. The Thai government has recognized the need to diversify the country's energy mix and reduce its dependence on fossil fuels. In recent years, Thailand has increased its use of renewable energy sources such as solar, wind, and hydropower. To prevent air pollution and global warming problems related to CO_2 emission, carbon capture and storage (CCS) in geological formations is currently a common procedure to reduce CO_2 emission in the atmosphere due to its large storage capacity and long-term storage solution [5, 6]. However, in Thailand, the CCS project has not been well established and developed. Therefore, preliminary studies on the potential rock formations and target areas are needed to develop the next step for the CCS project in Thailand.

Petroleum reservoirs are usually the main CO_2 geological storage targets compared with other geological storages. There are several advantages to store CO_2 in petroleum reservoirs including known geological structure, storage capability, sealed rock capacity, supported facilities, and economic benefits [5]. In addition, depleted gas reservoirs are considered good CO_2 storage due to their long-term capacity of holding gas [7, 8]. Petroleum reservoirs in Thailand are mainly located in offshore areas and are mainly sandstone reservoirs. However, the CO_2 point sources such as power and petroleum refineries are in onshore areas. Hence, onshore petroleum reservoirs may be more suitable and economical for onshore CO_2 storage sites [9]. The Khorat plateau, one of the most CO_2 point source areas in Thailand, is the main gas field produced from carbonate reservoirs.

There were few geological CO_2 storage studies on carbonate reservoirs in Thailand. Thus, it is meaningful and necessary to evaluate the feasibility of geological CO_2 storage in a carbonate reservoir. Moreover,

during CO_2 injection into a carbonate reservoir, CO_2 could be mixed with the reservoir fluid leading to chemical and mechanical changes in the reservoir. The changes could cause dissolution, precipitation, or corrosion in the reservoir; and these activities might improve or reduce the reservoir permeability and porosity [5, 8, 10–12]. These changes could significantly affect the safety, the storage capacity, and the seal capacity of geological CO_2 storages. In depleted carbonate reservoirs, the reservoir formation would be assumed to be saturated with water. Since carbonate minerals such as calcite and dolomite in the carbonate reservoirs do not react with anhydrous CO_2, so they could be dissolved by carbonic acid when injected CO_2 mixed with water in the reservoir [13, 14].

Nowadays, CO_2-water-rock interaction studies in sandstone reservoirs have been widely investigated, while carbonate reservoirs have not been well studied [6, 14–16]. To better understand the change in carbonate reservoirs and the geochemical reactions during CO_2 injection, CO_2-water-rock interaction experiment was setup for the carbonate rock samples from the Pha Nok Khao (PNK) Formation, a proven reservoir in the Khorat Plateau. This study also investigated changes in the potential seal rock samples from the Huai Hin Lat (HHL) Formation.

The purpose of this study was to evaluate the porosity changes in the rock samples due to chemical reactions by using X-ray diffraction (XRD), X-ray fluorescence (XRF), Inductively Coupled Plasma-Optical Emission Spectrometer (ICP-OES), and petrography. Thus, an experiment of soaking the rock samples in synthetic brine water for a CO_2-brine-rock interaction experiment was set up; changes in the samples were investigated. The results could help engineers and geologists understand and evaluate the feasibility and the safety of geological CO_2 storages in carbonate gas reservoirs in Thailand and adjacent regions.

MATERIALS AND METHODS

The Khorat Plateau with a total area of 560,000 km^2 contains two gas fields, Nam Phong and Sin Phu Horm. Natural gas has been produced from the fractured and dolomitized Permian carbonate reservoirs of the PNK Formation. The produced gas has been delivered to the Nam Phong Power Plant (Fig. 1). The Nam Phong and the Sin Phu Horm gas fields are located in the northwest and southeast of the power plant, respectively. The petroleum trap and reservoir of these two gas fields are a brachy-anticline with thrust faults and dolomitization at depths of about 1200 m to 1600 m. The main seals are siliciclastic rocks of the HHL Formation such as sandstone, mudstone and shale. However, there are several potential petroleum fields in the Khorat Plateau such as Dong Mun and Si That that have not yet been in production. These fields share similar geological structures with Nam Phong and Sin Phu Horm fields [9].

The PNK Formation overlies unconformably on the Devonian-Early Carboniferous rocks and mainly consists of carbonate rocks with minor siliciclastic rocks [17]. The PNK Formation is deposited in a shallow-marine carbonate platform various in lithological facies and is extensively distributed in the Khorat Plateau. Late Triassic extension event caused the development of localized half-graben structures that were then filled by Triassic sediments, which are preserved as the HHL Formation [18–20]. The HHL Formation is divided into two major units, the lower and the upper sequences [21]. The lower sequence consists of volcanic rocks, volcanic clastic rocks, conglomerates with some intercalations of limestone, sandstone, and shale beds [21]. The upper sequence mainly comprises sandstone, calcareous and carbonaceous shale, and argillaceous limestone with fossils [21]. The samples were selected based on different lithological facies from both reservoir and seal rock Formations including six samples from the PNK Formation and two samples from the HHL Formation (Fig. 1).

Preparation of experimental samples

Cubic-shaped rock samples were prepared with dimensions of approximately 2.5 cm × 2.5 cm × 2.5 cm and were applied in a static experiment (closed system) to increase the contact area between the rock surface and brine water (Fig. 2; [22]). It should be noted that three sets of cubic rock samples were prepared for this study. Each set contained eight rock samples from different lithologies or locations (Figs. 1 and 2). One set of the cubic rock samples was ground into powder for XRD and XRF analyses; the other was tested in the static experiment with CO_2-dissolved in synthetic brine water. Petrographic study was performed to observe the mineral composition and texture of the samples. Chemical changes in the synthetic brine water were also investigated to confirm the mineral dissolutions from the rock samples.

The sample powders (20 g each) were dried at 60 °C for 3 h. Major oxides (CaO, MgO, SiO_2, Al_2O_3, FeO_t, K_2O, Na_2O, MnO, TiO_2, and P_2O_5) were then analyzed using an X-ray fluorescence (XRF) spectrometer at the Department of Geology, Chulalongkorn University. This XRF examination was conducted at 60 kV/50 mA. The precession level of major oxide data exceeded 0.01%. At the same location, X-ray diffraction (XRD) analysis was conducted with a Bruker AXS D8 advanced diffractometer equipped with a copper-target tube and operating at 40 kV and 30 mA. The sample powders were scanned between 5 and 80° 2θ with 0.02° increments. The semi-quantitative XRD analysis was based on X-ray powder diffraction, and the Bruker EVA® software was integrated with the ICDD database of minerals. The first step was mineral identification, followed by the manual scaling of each

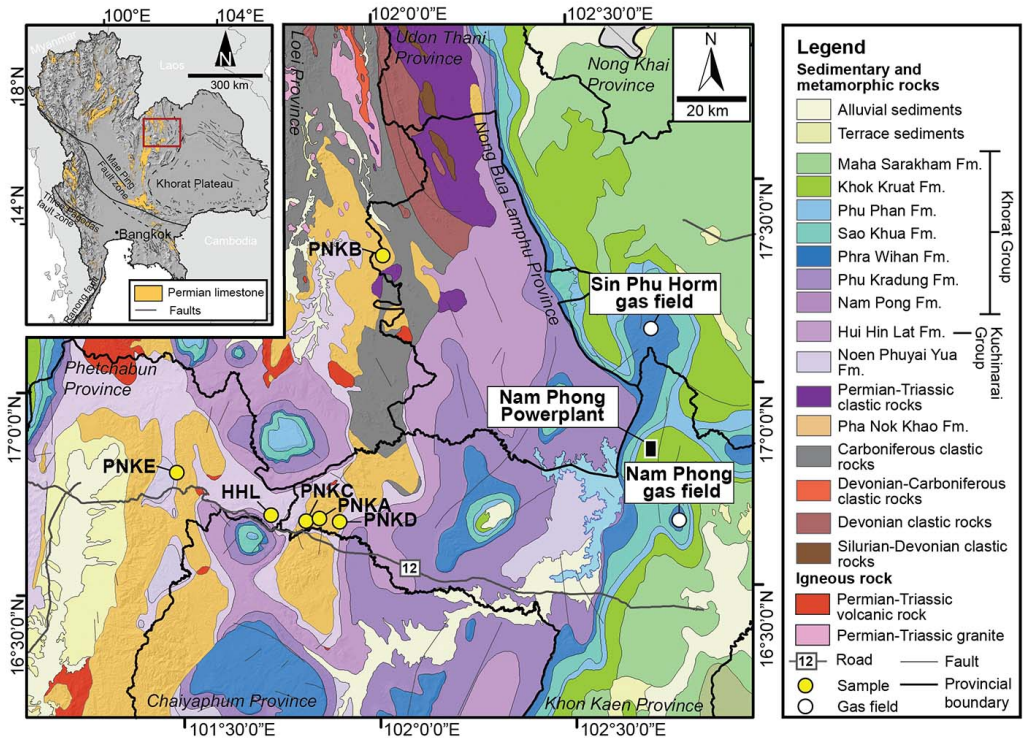

Fig. 1 Generalized geological map of the study area and sample locations. Samples were collected from the PNK and the HHL Formations. The map was obtained from the Department of Mineral Resources, from which the formations were modified from [31].

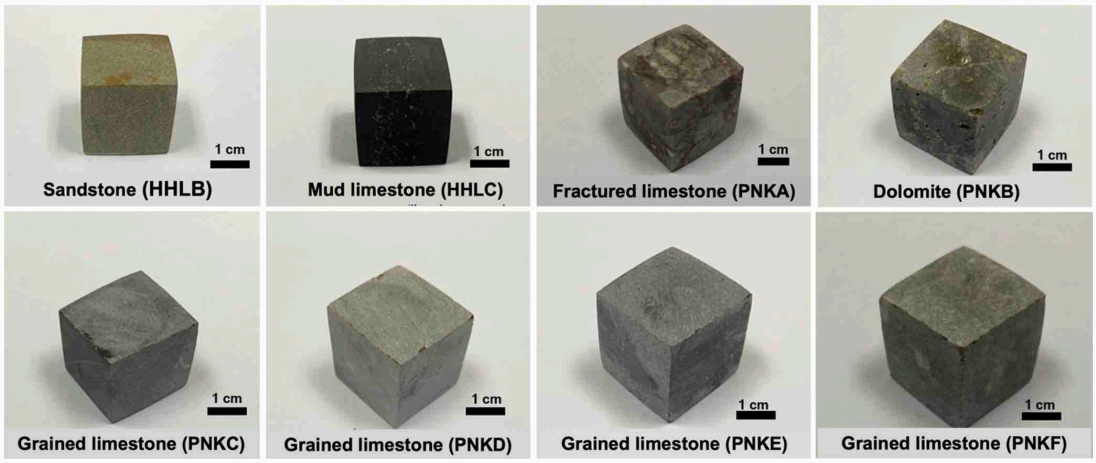

Fig. 2 Three sets of cubic rock samples (2.5 cm × 2.5 cm × 2.5 cm) were prepared, including fractured limestone, grained limestone, mud limestone, dolomite, and sandstone from the PNK and the HHL Formations.

mineral's peaks to provide the best fit to the observed XRD diffractogram. Using the Bruker EVA® software, the percentage of minerals was converted from an area calculation where there was a unique peak in the interval. The computation area was performed between two points (entry points) of the peak, which determines the peak's maximum height and net area.

The total porosity of the rock samples was determined using liquid pycnometer techniques based on Tiab and Donaldson [23]. The sample was weighed in air, and then weighed again after being fully immersed in water. Thus, the volume and density of the solid

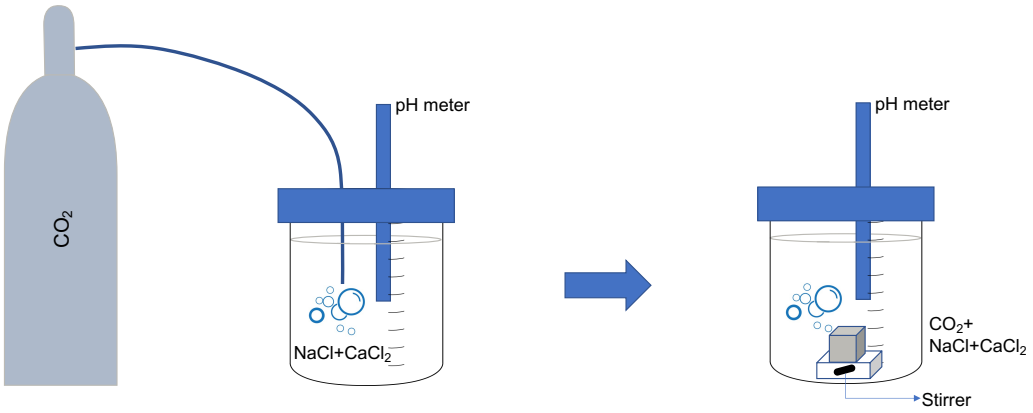

Fig. 3 Schematic diagram for the static CO_2-brine-rock interaction experiments. The rock samples were analyzed at one-, two-, and four-week intervals.

grains within the rock samples could be determined. The total volume of the rock samples was calculated from the measurements of the samples' dimension, and the volume of the pores was obtained from the difference between the total volume of the rock and the volume of the solid grains [23].

Porosity changes due to CO_2-induced geochemical reactions were investigated by comparing changes in the rock samples before and after being soaked in the synthetic brine water. The samples were prepared by continuous exposure to the synthetic brine water. The soaking experimental setup was shown in Fig. 3.

Synthetic CO_2-brine water preparation

Synthetic brine water was prepared by mixing 268.8 g of NaCl and 571.4 g of $CaCl_2$ with 1,000 ml deionized water (Type-I) to obtain a saline with a concentration of 9.75 mM and a measured pH of 5.6. Then, 400 ml of the prepared brine water was transferred to a test vessel. Compressed CO_2 (99.95%) was introduced into the brine at a rate of 0.1 normal liter per minute at 25 °C and a pressure of 100 kPa for 6 h to dissolve CO_2 into the brine. When saturated, the CO_2-brine was an acidic solution with a measured pH of 3.55. Details of synthetic CO_2-brine preparation was reported in Thanasaksukthawee et al [24].

Experimental procedure

Cubic rock samples were washed with deionized water, dried at 105 °C for 48 h [25], and individually weighed. Each sample was loaded into the test vessel containing 400 ml of 9.75 mM CO_2-brine solution and a stirrer. The temperature was maintained at room temperature (25 °C) under a pressure of 100 kPa. During the experiment, the solution was stirred for 6 hours a day to speed up the reaction rate. After each experiment interval (1, 2 and 4 weeks), the soaked cubic samples were retrieved, rinsed repeatedly with distilled water, dried at 60 °C for 24 h, and weighed.

Brine water from each experiment (before and after soaking of sample) was analyzed by Inductively Coupled Plasma-Optical Emission Spectrometer (ICP-OES model Agilent G8018A) at the Center of Excellence on Hazardous Substance Management, Chulalongkorn University. Concentrations of major elements (i.e., Al Ca, Mg, Si, Na, and Mn) in the brine water were analyzed and compared.

RESULTS

Petrographic investigation

The mineral compositions and textures of the eight samples were confirmed with the classification for PNK and HHL Formations (Fig. 4). The samples were, then, classified into five lithological facies including fractured limestone, grained limestone, mud limestone, dolomite, and sandstone.

The fractured limestone sample (PNKA) was mainly composed of calcite with various sizes of fractures (Fig. 4a). The fractures were filled with iron oxide staining and hosted rock fragments. The dolomite (PNKB) sample mainly consisted of dolomite crystals (Fig. 4b). The dolomite crystals appeared as a rhomb shape with gaps between crystals. The grained limestones (PNKC, PNKD, PNKE, and PNKF) were mainly composed of bioclasts and peloids (Fig. 4c-f). The bioclasts or fossils varied in size and were mostly filled with sparry calcite. Microfractures and veins were common in these grained limestone samples. The PNKD was mainly characterized by calcite crystals, while the PNKF showed significant dolomite crystals. Large bioclasts were dominated in the PNKE. The porosities in these PNK samples were various depending on the occurrence of intragranular and framework porosities in their bioclasts.

The sandstone sample (HHLB) consisted of quartz,

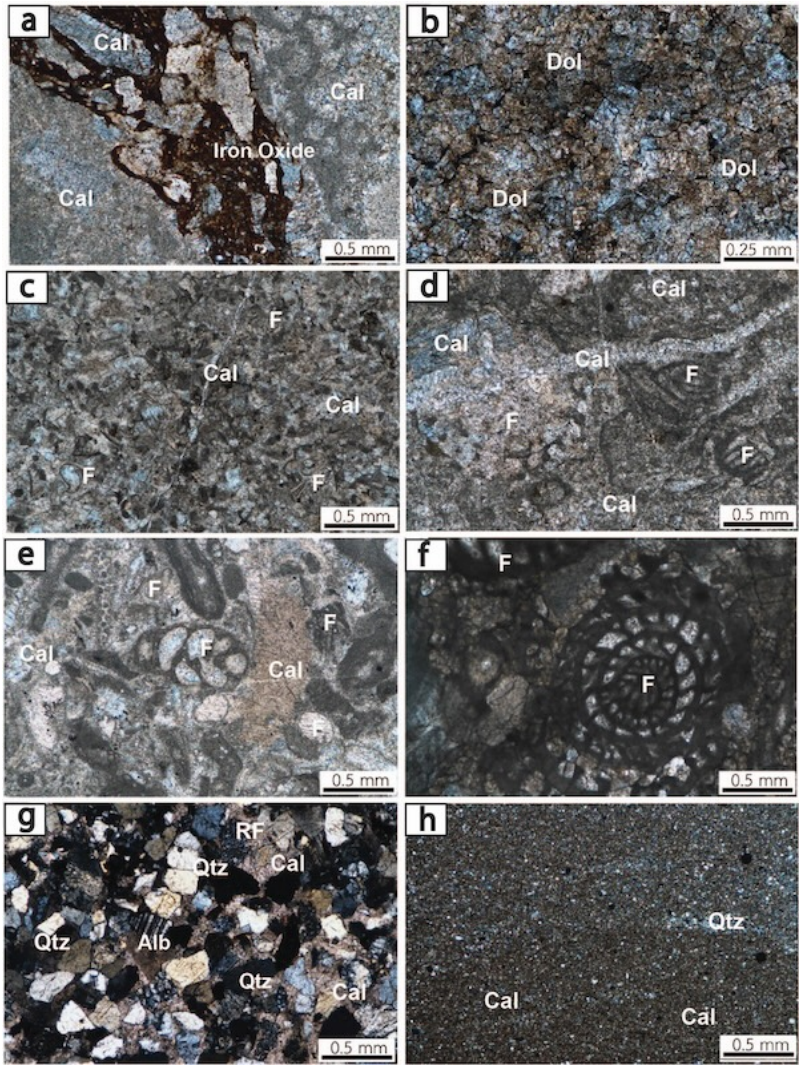

Fig. 4 Microscopic photographs under cross-polarized light of the rock samples from the PNK and the HHL Formations. (a), fractured limestone (PNKA) filled with iron oxide staining; (b), dolomite (PNKB) with crystalline dolomite rhombs; (c), grained limestone (PNKC) with bioclasts and micro-veins; (d), grained limestone (PNKD) with bioclasts and micro-veins; (e), grained limestone (PNKE) with bioclasts filled by calcite; (f) ,vgrained limestone (PNKF) with fossils corroded by stylolite; (g), sandstone (HHLB) with calcareous cement; and (h),vmud limestone (HHLC) very fine grain calcite. Note for the abbrevations: Cal, calcite; Dol, dolomite; F, fossil; RF, rock fragment; Qtz, quartz; and Alb, albite.

feldspar, and rock fragments with moderate sorting (Fig. 4g). The grain size in the sandstone was about 0.1–0.4 mm with calcareous cement. The grain shape was angular to subround with low porosity. The mud limestone sample (HHLC) consisted of very fine grains including clay and calcite minerals (Fig. 4h). The HHLC sample had low porosity without micro fractures and veins.

Change in mineral composition

Detailed mineral compositions of samples from XRD data, before and after soaking. were presented in Table 1. Before soaking, the carbonate rock samples from both Formations were dominated by calcite (0.67–99.58 %) and dolomite (0.50–99.33 %), with minor quartz (0.29–7.73 %) in some samples. It should be noted that the mineral composition in the dolomite (PNKB) mainly consisted of dolomite, with minor calcite, while the sandstone (HHLB) mainly consisted of quartz with minor calcite due to calcareous cementation. In addition, chlorite, illite, and plagioclase (albite) were only detected from the HHL samples.

In general, the proportion of the sample's mineral composition was changed after soaking in the brine water. In addition, the change in the mineral compositions of the carbonate samples was different between

Table 1 Mineral compositions (%) of the rock samples before and after week four of the CO_2-brine-rock interaction experiments.

Mineral		Fractured Limestone	Dolomite	Grained limestone	Grained limestone	Grained limestone	Grained limestone	Sandstone	Mud limestone
		PNKA	PNKB	PNKC	PNKD	PNKE	PNKF	HHLB	HHLC
Calcite	Before	99.58	0.67	98.16	99.50	99.18	69.39	15.74	11.30
	After	99.45	0.46	99.72	99.93	98.37	71.63	23.76	9.69
Dolomite	Before	–	99.33	0.74	0.50	0.53	30.61	–	46.59
	After	–	99.54	0.23	0.07	1.30	28.19	–	64.71
Quartz	Before	0.42	–	1.10	–	0.29	–	73.87	7.73
	After	0.55	–	0.05	–	0.33	0.18	68.96	4.96
Albite	Before	–	–	–	–	–	–	–	32.45
	After	–	–	–	–	–	–	5.67	19.85
Chlorite	Before	–	–	–	–	–	–	1.02	–
	After	–	–	–	–	–	–	1.61	–
Illite	Before	–	–	–	–	–	–	–	1.92
	After	–	–	–	–	–	–	–	0.80

Table 2 Major elements (wt.%) of the rock samples before and after week four of the CO_2-brine-rock interaction experiments.

Sample		CaO	MgO	SiO_2	Al_2O_3	FeO_t	TiO_2	K_2O	Na_2O
PNKA	Before	93.35	0.54	3.74	1.88	0.30	0.06	0.04	0.00
	After	95.20	0.69	2.54	1.11	0.36	0.03	0.03	0.00
PNKB	Before	65.28	34.66	0.00	0.06	0.00	0.00	0.00	0.00
	After	60.61	39.33	0.03	0.00	0.03	0.00	0.00	0.00
PNKC	Before	94.89	1.48	2.30	0.55	0.00	0.00	0.04	0.00
	After	98.34	1.26	0.27	0.06	0.03	0.00	0.00	0.00
PNKD	Before	99.05	0.91	0.04	0.00	0.00	0.00	0.00	0.00
	After	98.78	1.04	0.07	0.03	0.04	0.00	0.00	0.00
PNKE	Before	97.14	1.59	1.01	0.24	0.00	0.00	0.01	0.00
	After	97.54	1.21	1.03	0.10	0.10	0.00	0.01	0.00
PNKF	Before	94.20	5.22	0.40	0.09	0.00	0.00	0.00	0.00
	After	92.99	6.11	0.61	0.14	0.09	0.00	0.00	0.00
HHLB	Before	11.44	1.11	78.45	0.00	5.56	0.47	0.33	1.73
	After	16.07	1.11	65.12	8.48	4.84	0.46	0.53	1.74
HHLC	Before	17.82	5.25	58.51	0.00	6.70	0.74	3.42	7.30
	After	18.86	7.98	45.56	13.74	4.54	0.51	2.74	5.85

limestone and dolomite. Calcite tended to decrease in the carbonate rocks due to dissolution in acidic water of CO_2-brine water as observed from PNKA, PNKB, and PNKE samples (Table 1). The dolomite mineral also tended to dissolve in the brine water. The dissolution of dolomite mineral was, sometimes, better than calcite in some samples such as PNKC, PNKD, and PNKF. The fractured limestone was characterized by a network of fractures and veins. Thus, calcite was easily dissolved in the fractured limestone sample leading to increasing in the percentage of quartz after soaking. The HHL samples showed a decrease in the proportion of quartz; thus, the solubility of quartz in these HHL samples tended to be better than that of calcite and dolomite (Table 1). It should be noted that dolomite mineral could form with both calcium (Ca) and magnesium (Mg) [26]. Hence, major elements from XRF analysis of the dolomite sample illustrated high concentrations in both Ca and Mg.

The major element analysis was to show the geochemical changes of the rock samples before and after soaking and to confirm the change in mineral compositions. Significant changes in major element concentrations in the samples were observed, as presented in Table 2. Before soaking, CaO concentrations were observed in all samples (11.44–17.82 wt.% in the HHL and 65.28–99.05 wt.% in the PNK), with a usually high value for the limestone samples. MgO concentrations varied from 0.54 to 34.66 wt.% and were high in the dolomite sample (PNKB). Consistent with the XRD analysis, other trace elements were also found in the PNK samples, such as SiO_2 (0.00–3.74 wt.%),

Al_2O_3 (0.00–1.88 wt.%), and FeO_t (0.00–0.30 wt.%). SiO_2 concentrations (58.51–78.45 wt.%) were mainly dominated in the HHL samples. Comparison between XRD and XRF data, it should be noted that the high SiO_2 concentration in the HHLC (mud limestone) came from the presence of quartz, plagioclase (albite) and clay minerals. An anomalous high FeO_t and Na_2O concentrations in the HHLC could be due to chlorite and plagioclase (albite) (Table 2).

Change in brine water chemistry

Major ions detected in the brine water were Ca, Mg, Si, and Na, and their concentrations increased with soaking time. The brine water was made from $CaCl_2$ and NaCl, hence the concentrations of Ca and Na were high at the beginning of the experiment. Table 3 shows the percentage changes of ions between before and after each soaking interval (1, 2, and 4 weeks). The highest percentage change was Mg followed in order by Si and Ca, while the lowest percentage change was the Na. Dolomite was the only source of Mg in the samples; thus, the increase in the concentration of Mg was mainly due to the dissolution of dolomite. Moreover, the chemical changes in the synthetic brine water coincided with the mineral and chemical compositions of the rock samples. Although, the sandstone (HHLB) showed no dolomite crystal from XRD analysis, XRF and ICP-OES analyses showed the presence of dolomite in the HHLB sample (Tables 2 and 3). The reason could be that the amount of dolomite crystals in the HHLB sample was too small to be detected by the XRD instrument. The dolomite (PNKB) and mud limestone (HHLC) samples were characterized by having dolomite in their compositions. As a result, Mg was detected in the brine water after soaking the samples (Table 3). However, it should be noted that the synthetic brine water was saturated with Ca; and the Ca saturation could affect the solubility of calcite in this study.

Change in bulk porosity

Before soaking, the PNK and the HHL samples showed total porosity ranging from 1.29% to 7.42% and 3.08% to 7.19%, respectively (Table 4). The effective porosity of the samples was normally lower than the total porosity. The effective porosity of the HHL samples (1.99%–2.17%) was higher than in the PNK carbonate samples (0.28%–1.34%). Significant differences between effective and total porosities were observed in the carbonate rocks, except the PNKD. The PNKD sample showed the effective porosity close to the total porosity indicating that most of the pores were connected within the sample. The connected pores allowed fluid to flow through all pore spaces of the sample, contributing to the highest change in bulk porosity after soaking of the PNKD sample (Table 4).

Once the samples immersed into the CO_2-brine solution, the porosities of the reservoir (PNK) and seal (HHL) rocks were increased depending on their lithological facies (Table 4). This was likely a major contribution from the mineral dissolution of rock samples in both Formations. After 4 weeks of soaking, the grained limestone sample (PNKD) had the highest total porosity change, followed in order by the fractured limestone (PNKA) and the grained limestone (PNKC). The sandstone sample (HHLB) also illustrated a significant increase in the total porosity change, while the mud limestone (HHLC) showed the lowest total porosity change in this study.

Generally, in nature, grained limestones comprised a lot of fossils or bioclasts, resulting in relatively high porosity compared with mud limestones. A large difference in total porosity among the grained limestones could happened when they were connected. In addition, fractures in limestone could increase the total porosity of the rock samples. Regarding the effective porosity, it was found that the grained limestones (PNKC and PNKD) had good effective porosity values. Fig. 4 shows the micro-fractures in the rock samples of PNKA, PNKC and PNKD which could increase porosity of the rock. Thus, total porosity was moderate to high in these samples. The dolomite (PNKB) sample showed a high total porosity but a low effective porosity causing the fluid not to flow easily through pore spaces. Therefore, the dissolution of minerals rarely occurred in the dolomite sample, and its porosity did not change much after soaking.

The HHL samples were deposited in a mixed siliciclastic-carbonate environment resulting in higher effective porosities compared with the PNK carbonate samples (Table 4). The sandstone (HHLB) showed a high total porosity but a moderate effective porosity due to calcareous cementation. Hence, fluids could flow within the rock contributing to the significant change in bulk porosity (Table 4). Meanwhile, the mud limestone (HHLC) had high total and effective porosity values. Fine-grained sediment rocks usually had narrow and complex pore networks resulting in low permeability [27, 28]. In this study, fluids could not flow easily with the mud limestone sample giving a little change in bulk porosity [27].

DISCUSSION

Mineral dissolution

The dissolution of minerals was mainly affected by the CO_2 dissolution in the low pH CO_2-brine solution. This study showed that dolomite, calcite, and quartz dissolved during CO_2 injection in carbonate formations. Based on geochemical analyses, magnesium (Mg) tended to dissolve more easily and at a faster rate than silicon (Si) and calcium (Ca) because the Mg ions are smaller and have a greater charge density than the silicon and the calcium ions, which allows them to form more stable complexes with water and other ions. This

Table 3 Changes in chemistry of the brine water at week-one, -two, and -four soaking intervals of the samples.

Sample	Week	Ca (%)	Mg (%)	Si (%)	Na (%)
PNKA	1	17.47	863.36	255.87	1.58
	2	11.20	594.43	131.08	1.45
	4	33.35	636.59	109.09	2.77
PNKB	1	14.61	13,832.00	78.17	1.82
	2	14.10	15,418.00	117.11	0.86
	4	26.81	30,816.00	51.48	2.04
PNKC	1	31.68	2,460.00	186.75	1.76
	2	26.34	1,869.00	223.38	1.54
	4	21.39	2,811.00	204.69	1.58
PNKD	1	76.34	3,287.00	203.32	4.09
	2	14.97	1,624.00	215.58	0.75
	4	15.41	1,279.00	179.57	0.86
PNKE	1	17.55	918.35	234.13	1.22
	2	22.59	779.70	127.59	1.68
	4	18.95	1,380.00	197.85	1.26
PNKF	1	26.77	4,633.00	171.25	2.34
	2	26.29	1,737.00	80.92	1.21
	4	19.12	1,714.00	94.98	1.28
HHLB	1	15.37	2,653.00	861.40	0.65
	2	14.38	957.07	535.55	1.10
	4	39.05	1,456.00	315.77	1.84
HHLC	1	9.23	22,897.60	965.64	0.77
	2	12.48	3,862.00	54.08	1.45
	4	19.86	40,086.00	188.38	2.31

Table 4 Changes in bulk porosity of the rock samples before the experiment and at week-one, -two, and -four soaking intervals.

Sample	Rock type	Effective	Total porosity (%)				Total
		porosity (%)	Before	Week 1	Week 2	Week 4	change (%)
PNKA	Fractured limestone	0.28	2.72	2.82	2.94	3.16	16.21
PNKB	Dolomite	0.86	7.42	7.46	7.50	7.67	3.51
PNKC	Grained limestone	1.34	3.25	3.37	3.43	3.56	9.68
PNKD	Grained limestone	1.28	1.29	1.51	1.55	1.65	27.46
PNKE	Grained limestone	0.68	7.19	7.26	7.32	7.42	3.14
PNKF	Grained limestone	0.52	6.82	6.84	6.95	7.11	4.26
HHLB	Sandstone	1.99	3.08	3.04	3.16	3.32	7.87
HHLC	Mud limestone	2.17	7.19	7.15	7.23	7.35	2.20

finding also coincides with other studies (e.g., [6]). Hence, CO_2-water-rock interaction in carbonate formations with strong heterogeneity could be complex. During CO_2 injection, the carbonate rocks were exposed to the low pH CO_2-brine water leading to the dissolution of minerals from dolomite, quartz, and calcite. The dissolution could alter the rock's mineral composition and physical properties over time [29]. In addition, after soaking, the dissolution of minerals left several micro-holes on the rock surfaces, confirming that the CO_2-water-rock interaction could cause geochemical and physical changes in rock formations. For example, it could affect the bulk porosity and the strength of a reservoir formation which was observed in a short-time lab experiment leading to fracture failure after hundreds of years of CO_2 injection.

The results of the XRD and XRF analyses of rock samples were different in mineral and geochemical changes after soaking. This might be caused by sample preparation when the rock samples were divided into three sets, with probably slightly different in mineral and geochemical characteristics of the rock samples. This problem was inevitable because the rock samples for XRD and XRF analyses needed to be crushed.

Control factors in CO_2-brine-rock interaction

From this study, the control factors in CO_2-brine-rock interactions of the carbonate rocks were lithology, rock formation brine water, and effective porosity.

The rock samples used in this study were sili-

ciclastic and carbonate rocks. The major mineral compositions and cementations in these rock samples were calcite and dolomite, which are easily dissolved in an acidic environment [13, 30]. Dolomite minerals may be formed by the replacement of the Ca ions by the Mg ions after lithification of sediments. It is a secondary dolomite, which causes limestones to have more gaps in the rock and may develop into pores or voids that can be observed with naked eyes, for example, PNKB. In addition, fractures and veins can increase CO_2-brine-rock interactions by allowing fluids to flow within the rock formation.

Rock formation brine water in the reservoir also plays an important role in CO_2-brine-rock interactions. Supposedly, a target reservoir was saturated with ions, and solubility depended on the degree of saturation of brine water or the degree of dissolved ions; the $CaCl_2$ and NaCl concentrations in the synthetic brine water in this study could affect the calcite dissolution in the samples. Consequently, the dolomite mineral was better dissolved in synthetic brine water compared with calcite due to high Ca saturation.

The results of this study demonstrated that effective porosity was the main control for fluid to flow, which greatly affected CO_2-brine-rock interactions within the rock formation. This allowed fluid to interact with rock surfaces, or mineral surfaces, thus causing more mineral dissolution and increasing gaps within the rock formation.

Potential for geological carbon storage

From this study, a carbonate reservoir might be not suitable for a long-term storage due to the dissolution in an acid environment after CO_2 injection. However, more experiments are needed to test this hypothesis in the future. The trapping mechanism in carbonate reservoirs was more likely a solubility trapping rather than a mineral trapping (e.g., [15]). Since the element concentrations in carbonate reservoirs change after CO_2 injection, long-term mineral precipitation, that might affect permeability of carbonate reservoirs, should be further investigated.

CONCLUSION

This study investigated the geochemical and physical changes in the rock samples (i.e., fractured limestone, dolomite, mud limestone, grained limestone, and sandstone) caused by CO_2-brine-rock interaction using petrography, petrography, XRD, XRF, and ICP-OES analyses. After soaking in CO_2-brine solution, most rocks presented an increased porosity due to the dissolution of the mineral composition in carbonate rocks. During CO_2 injection, carbonate rocks were exposed to the low pH CO_2-brine solution leading to the dissolution of minerals from dolomite, quartz, and calcite. In this study, control factors in CO_2-brine-rock interactions of the carbonate rocks were lithology, rock formation brine water, and effective porosity. Based on the findings, the PNK carbonate reservoir might be not suitable for long-term storage due to the dissolution in an acid environment after CO_2 injection. The dissolution could affect the bulk porosity and strength of a reservoir formation which was observed in a short-time lab experiment leading to fracture failure after hundreds of years of CO_2 injection.

Acknowledgements: The authors gratefully acknowledge the financial support from the National Research Council of Thailand (NRCT) under Grant Number RES_65_344_23_031. Reviewers are thanked for their useful and constructive comments.

REFERENCES

1. IEA (2020) World Energy Outlook 2020, IEA, Paris. Available at: https://www.iea.org/reports/world-energy-outlook-2020.
2. Bai M, Sun J, Song K, Reinicke KM, Teodoriu C (2015) Evaluation of mechanical well integrity during CO_2 underground storage. *Environ Earth Sci* **73**, 6815–6825.
3. Kibria A, Akhundjanov SB, Oladi R (2019) Fossil fuel share in the energy mix and economic growth. *Int Rev Econ Financ* **59**, 253–264.
4. Lott MC, Pye S, Dodds PE (2017) Quantifying the co-impacts of energy sector decarbonisation on outdoor air pollution in the United Kingdom. *Energy Policy* **101**, 42–51.
5. Tang Y, Hu S, He Y, Wang Y, Wan X, Cui S, Long K (2021) Experiment on CO_2-brine-rock interaction during CO_2 injection and storage in gas reservoirs with aquifer. *Chem Eng J* **413**, 127567.
6. Ahmat K, Cheng J, Yu Y, Zhao R, Li J (2022) CO_2-water-rock interactions in carbonate formations at the Tazhong Uplift, Tarim Basin, China. *Minerals* **12**, 635.
7. Shukla R, Ranjith P, Haque A, Choi X (2010) A review of studies on CO_2 sequestration and caprock integrity. *Fuel* **89**, 2651–2664.
8. Peter A, Yang D, Eshiet KIII, Sheng Y (2022) A review of the studies on CO_2-brine-rock interaction in geological storage process. *Geosciences* **12**, 168.
9. Chenrai P, Jitmahantakul S, Bissen R, Assawincharoenkij T (2022) A preliminary assessment of geological CO_2 storage in the Khorat Plateau, Thailand. *Front Energy Res* **10**, 909898.
10. Mohamed IM, He J, Nasr-El-Din HA (2011) Permeability change during CO_2 injection in carbonate aquifers: Experimental study. In: *SPE Americas E&P Health, Safety, Security, and Environmental Conference*, OnePetro.
11. Adam L, MacFarlane J, van Wijk K, Shragge J, Higgs K (2015) Monitoring how carbonate cement dissolution affects rock frame properties due to CO_2 injection. In: *Presented at the Third International Rock Physics Meeting*.
12. Ilgen AG, Newell P, Hueckel T, Espinoza DN, Hu M (2019) Coupled chemical-mechanical processes associated with the injection of CO_2 into subsurface. In: *Science of Carbon Storage in Deep Saline Formations*, Elsevier, pp 337–359.
13. Wang X, Alvarado V, Swoboda-Colberg N, Kaszuba JP (2013) Reactivity of dolomite in water-saturated supercritical carbon dioxide: Significance for carbon capture

and storage and for enhanced oil and gas recovery. *Energ Convers Manage* **65**, 564–573.
14. Siqueira TA, Iglesias RS, Ketzer JM (2017) Carbon dioxide injection in carbonate reservoirs: A review of CO_2-water-rock interaction studies. *Greenh Gases Sci Technol* **7**, 802–816.
15. Azin R, Mehrabi N, Osfouri S, Asgari M (2015) Experimental study of CO_2-saline aquifer-carbonate rock interaction during CO_2 sequestration. *Proced Earth Plan Sci* **15**, 413–420.
16. Lu J, Mickler PJ, Nicot JP, Yang C, Darvari R (2016) Geochemical impact of O_2 impurity in CO_2 stream on carbonate carbon-storage reservoirs. *Int J Greenh Gas Con* **47**, 159–175.
17. Burrett C, Zaw K, Meffre S, Lai CK, Khositanont S, Chaodumrong P, Udchachon M, Ekins S, et al (2014) The configuration of Greater Gondwana-Evidence from LA ICPMS, U-Pb geochronology of detrital zircons from the Palaeozoic and Mesozoic of Southeast Asia and China. *Gondwana Res* **26**, 31–51.
18. Cooper MA, Herbert R, Hill GS (1989) The structural evolution of Triassic intermontane basins in northeastern Thailand. In: *Proceedings of the International Symposium on Intermontane Basins: Geology and Resources*, Thailand, pp 231–242.
19. Sattayarak N, Srilulwong S, Pum-Im S (1989) Petroleum potential of the Triassic pre-Khorat intermontane basin in Northeastern Thailand. In: *Proceeding of the International Symposium on Intermontane Basins: Geology and Resources*, Thailand, pp 43–58.
20. Booth J, Sattayarak N (2011) Subsurface carboniferous-cretaceous geology of northeast Thailand. In: Ridd MF, Barber AJ, Crow MJ (eds) *The Geology of Thailand*, Geological Society of London, UK, pp 185–222.
21. Chonglakmani C, Sattayarak N (1978) Stratigraphy of the Huai Hin Lat Formation (upper Triassic) in Northeastern Thailand. In: *Proceedings of the Regional Conference on Geology and Mineral Resources of Southeast Asia*, Thailand, pp 739–762.
22. Ali AH, Kandeel AM, Ouda AS (2013) Hydration characteristics of limestone filled cement pastes. *Chem Mater Res* **5**, 68–73.
23. Tiab D, Donaldson EC (2015) *Petrophysics: Theory and Practice of Measuring Reservoir Rock and Fluid Transport Properties*, Gulf Professional Publishing.
24. Thanasaksukthawee V, Santha N, Saenton S, Tippayawong N, Jaroonpattanapong P, Foroozesh J, Tangparitkul S (2022) Relative CO_2 column height for CO_2 geological storage: a non-negligible contribution from reservoir rock characteristics. *Energy Fuel* **36**, 3727–3736.
25. Lisci C, Pires V, Sitzia F, Mirao J (2022) Limestones durability study on salt crystallisation: An integrated approach. *Case Stud Constr Mater* **17**, e01572.
26. Mehmood M, Yaseen M, Khan EU, Khan MJ (2018) Dolomite and dolomitization model: A short review. *Int J Hydro* **2**, 549–553.
27. Pang X, Wang G, Kuang L, Li H, Zhao Y, Li D, Zhao X, Wu S, et al (2022) Insights into the pore structure and oil mobility in fine-grained sedimentary rocks: The Lucaogou Formation in Jimusar Sag, Junggar Basin, China. *Mar Petrol Geol* **137**, 105492.
28. Liu X, Lai J, Fan X, Shu H, Wang G, Ma X, Liu M, Guan M, et al (2020) Insights in the pore structure, fluid mobility and oiliness in oil shales of Paleogene Funing Formation in Subei Basin, China. *Mar Petrol Geol* **114**, 104228.
29. Akono AT, Druhan JL, Dávila G, Tsotsis T, Jessen K, Fuchs S, Crandall D, Shi Z, et al (2019) A review of geochemical-mechanical impacts in geological carbon storage reservoirs. *Greenh Gases Sci Technol* **9**, 474–504.
30. Deng H, Ellis BR, Peters CA, Fitts JP, Crandall D, Bromhal GS (2013) Modifications of carbonate fracture hydrodynamic properties by CO_2-acidified brine flow. *Energy Fuels* **27**, 4221–4231.
31. DMR (1985) *Geological Map of Thailand, Scale 1:250,000*, Geological Survey Division, Department of Mineral Resources, Bangkok.